

Room-temperature emission of highly excited GaAs/Ga_{1-x}Al_xAs quantum wells

E. Lach and A. Forchel

4. Physikalisches Institut, Universität Stuttgart, Pfaffenwaldring 57, D 7000 Stuttgart 80, Federal Republic of Germany

D. A. Broido* and T. L. Reinecke

Naval Research Laboratory, Washington, D.C. 20375

G. Weimann and W. Schlapp†

W. Schottky Institut, Garching, Federal Republic of Germany

(Received 20 February 1990)

The emission spectra of GaAs/Ga_{1-x}Al_xAs quantum wells were studied under high optical excitation at room temperature. Mesa structures 50 μm in size were used to confine the electron-hole carrier system laterally and thus to produce a uniform high density of carriers. Carrier densities were sufficient to fill the quantum well to the top of the Ga_{1-x}Al_xAs barrier, and electron subbands up to $n=3$ were filled. Accurate values of the densities and temperatures were obtained by fitting the spectra using calculations of the full coupled valence bands for the hole dispersion relations and for the optical matrix elements. The resulting band-gap renormalizations were found to depend on the subband index. Theoretical results based on an extension of the local-density approach are presented which are consistent with the observed subband dependence of the band-gap renormalization.

Many-body effects in the optical and thermodynamic properties of highly excited semiconductors have been studied extensively in the past two decades both experimentally and theoretically. Recently, the effects of reducing dimensionality from three dimensions (3D) to two dimensions (2D) has been addressed through studies of quantum-well systems. One many-body effect of particular interest is the reduction of the band gap due to exchange-correlation effects at finite carrier densities. A substantial increase of the band-gap renormalization has been reported¹ in this (quasi-2D) system as compared to the 3D case. Very recently experimental results have been reported² in the In_xGa_{1-x}As/InP system for small mesa structures, which give good carrier homogeneity. In this latter work a dependence of the band-gap renormalization on the subbands involved in the transition was observed.

In order to obtain accurate values of the carrier densities and temperatures, detailed fits to the emission line shapes must be done. For quantum wells with well widths on the order of 100 Å the strong coupling between the heavy- and light-hole bands gives strong nonparabolicities in the dispersions of the valence bands parallel to the quantum well.^{3,4} The coupling also modifies the electron-hole matrix elements and can make transition probabilities finite which otherwise would have been forbidden. For carrier densities involved in high-excitation experiments, states which are strongly modified by these valence-band couplings are filled. To date, no analysis of emission line shapes, including the effects of these strong couplings, has been performed.

In this work, room-temperature emission experiments involving high-density electron-hole plasmas have been performed on a 10.3-nm GaAs/Ga_{0.63}Al_{0.37}As quantum well. Mesa structures were used to confine the plasma laterally and to give highly homogeneous high-density carrier systems. In this work, accurate values of the carrier

densities and temperatures were determined by performing line-shape fits using calculations of the full nonparabolic dispersions of the coupled valence bands and also the corresponding optical matrix elements. As a result, high quality fits to the data were obtained. From these analyses it has been found in detail that the band-gap renormalizations depend on the subbands involved in the transitions. Here we also present theoretical results based on a two-component generalization of the local-density approximation for the exchange-correlation energy which gives subband-dependent band-gap renormalizations which are qualitatively consistent with experiment.

Great care was taken to study the electron-hole plasma emission under spatially homogeneous conditions. In order to confine the carrier system laterally, mesa structures with dimensions ranging from 20×20 μm² to 200×200 μm² were prepared by optical lithography and etching. Prior to the measurements, the lateral surfaces of the mesas were passivated by Na₂S:H₂O to avoid any significant density gradient due to recombination at the etched side walls. Because of the high surface-recombination velocity of GaAs (~10⁷ cm/s) (Ref. 5) the passivation step is essential to provide a laterally homogeneous density. In particular, the passivation permits reduction of the excitation power by 1–2 orders of magnitude as compared to mesas which were only etched.

The samples were excited by 100-ns pulses of a Q-switched frequency-doubled Nd-doped yttrium aluminum garnet laser (λ = 532 nm, repetition rate = 10 kHz) with peak powers $P_{exc} \leq 65$ kW/cm². The emission was spectrally dispersed by a 0.85-m double monochromator and detected by a GaAs photomultiplier interfaced with a fast single-photon counting system. The spectra reported here were obtained using a 10-ns gate positioned at the maximum of the excitation pulse.

Figure 1 shows a series of spectra recorded at different

excitation intensities between 1.6 and 65 kW/cm². For the lowest excitation intensity, the emission corresponds to a relatively narrow feature centered at about 1.46 eV. This feature is due to transitions between the first electron subband and the first heavy- and light-hole valence bands, which are denoted 1e-1hh and 1e-1lh, respectively. With increasing excitation, the emission intensity increases predominantly on the high-energy side, and a pronounced peak due to transitions between the second subbands appears. In addition to the band-filling effects, the low-energy edges of the emission lines show redshifts due to many-body renormalization of the band gap.

If the excitation power is increased above about 65 kW/cm² the emission spectra show no further significant changes up to the damage threshold of the samples — except for a weak decrease of the slope of the high-energy edge of the spectra. In particular, the integrated emission intensity and the half-width saturate. Due to the light conduction-band mass of the GaAs, the width in en-

ergy of the spectra is given mainly by band filling in the conduction-band potential well. Using a conduction-band discontinuity of 65% and the Al content of the barriers of 37%, we obtain a conduction-band well depth of 290 meV. This value is significantly lower than the energy width of the emission at the highest excitation powers (1.36–1.72 eV). This indicates that for the highest excitation-level states in the conduction-band potential well up to the barrier level are occupied. A further increase of the excitation power therefore results in the occupation of states in the Al_xGa_{1-x}As barrier which do not give rise to emission in the energy range of the quantum well.

In order to determine quantitatively the carrier density, the temperature and band-gap renormalization from the measured spectra, we have performed detailed numerical fits to the emission spectra. The spontaneous emission of the quasi-2D electron-hole plasma at energy $\hbar\omega$ is given by

$$I(\hbar\omega) \sim \omega^2 \sum_{i,j} \int_{E_i^0}^{\infty} \int_{E_j^0}^{\infty} |M_{ij}|^2 D(E_i, E_j) f_e(E_i) f_h(E_j) \delta_{\Gamma}(E_i + E_j + E_g - \hbar\omega) dE_i dE_j, \quad (1)$$

$$D(E_i, E_j) = \oint_{l(k)} \frac{dl}{|\nabla_k [E_i(k) + E_j(k)]|}.$$

Momentum is taken to be conserved in the electron-hole recombination in Eq. (1) with $\mathbf{k} = \mathbf{k}_e = \mathbf{k}_h$ and $D(E_i, E_j)$ is the joint density of states. E_i and E_j are the electron and hole dispersions, where E_i^0 and E_j^0 are the electron- and hole-subband bottoms. $M_{ij}(E_i, E_j)$ is the optical matrix

element which, in general, depends on the hole energy as a result of valence-band coupling. The sum over all i, j is taken over all confined subbands. f_e and f_h are the electron and hole Fermi functions, and E_g is the bulk band gap. $\delta_{\Gamma}(E)$ includes a broadening of the transitions due to intravalley relaxation effects using the method due to Landsberg.⁶

In previous work, emission line shapes have been fitted neglecting the valence-band-mixing effects.^{1,2,7} Constant optical matrix elements and arbitrary choices for the parabolic heavy- and light-hole bands have been used. In this work we have made detailed numerical calculations of the nonparabolic dispersions of the hole bands and of the optical matrix elements using the subband $\mathbf{k} \cdot \mathbf{p}$ method.⁴ We find strong nonparabolicities in the hole dispersions and energy dependences in the optical matrix elements for energies needed to fit the emission lines observed here.

The solid line in Fig. 2(a) shows a line-shape fit to an experimental spectrum (dotted line) recorded at an excitation power of 22 kW/cm². The overall agreement of the experimental and calculated emission line shapes is satisfactory. The center section of Fig. 2 displays the contributions of the transitions involving the several different subbands to the emission. The allowed transitions ($\Delta n = 0$, solid lines) show significant effects due to valence-band coupling; for comparison, for parabolic uncoupled hole bands, each contribution in Fig. 2(b) would fall off smoothly with the Fermi functions for increasing energy. For the quantum well studied here, for example, the valence-band coupling causes a shoulder at about 1.5 eV in the 1e-1hh spectrum and a maximum 25 meV above the subband edge of the 1e-1lh transition energy.

The dashed lines in Fig. 2(b) correspond to forbidden intersubband transitions ($\Delta n = 1$) which become allowed due to valence-band coupling. There is strong contribution from transitions between the second conduction sub-

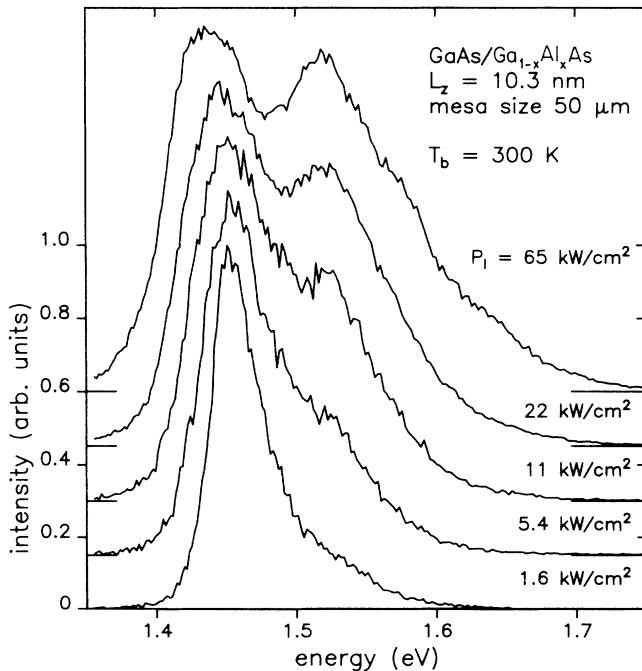


FIG. 1. Luminescence spectra of a 10.3-nm GaAs/Ga_{0.63}Al_{0.37}As quantum well for different excitation powers. In order to obtain a laterally homogeneous density distribution, the spectra are taken from a 50×50 μm² mesa structure with passivated side walls. For clarity the spectra have been displaced vertically, as indicated by horizontal bars.

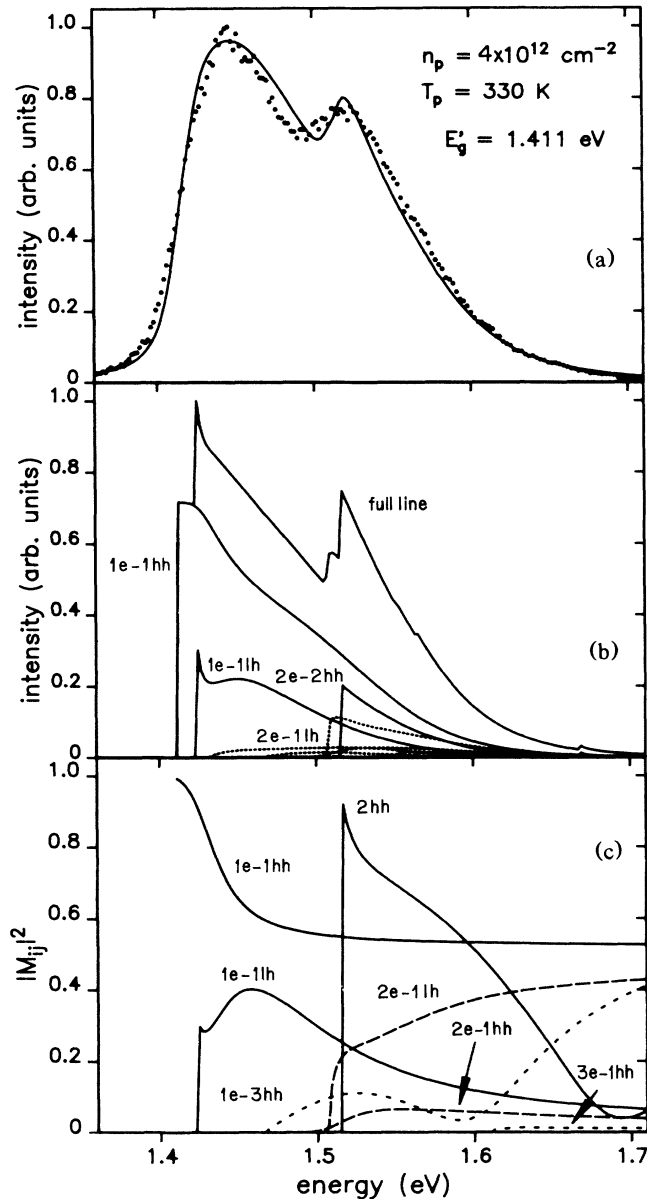


FIG. 2 (a) Line-shape fit of an experimental high-excitation spectrum (points). The plasma density, temperature, and the band gap are indicated. (b) Contributions of allowed (solid lines) and forbidden transitions (dashed lines) to the calculated spectrum. (c) Energy dependence of the matrix elements for different transitions.

band and the first light-hole valence band $2e-1lh$. In addition, the $1e-2hh$, $1e-2lh$, and the $2e-1hh$ transitions contribute significantly. On the other hand, the contributions from the parity allowed, forbidden transitions ($\Delta n = 2, 4, \dots$) are small as a result of small matrix elements for these transitions and small population factors for the higher-index subband.

Figure 2(c) shows the calculated matrix elements for the $1e-1hh$, $1e-1lh$, and $2e-2hh$ transitions (solid lines), those for the forbidden $2e-1lh$ and $2e-1hh$ (dashed lines) transitions, and those for the parity-allowed forbidden transitions $1e-3hh$ and $3e-1hh$ (dotted lines). We note

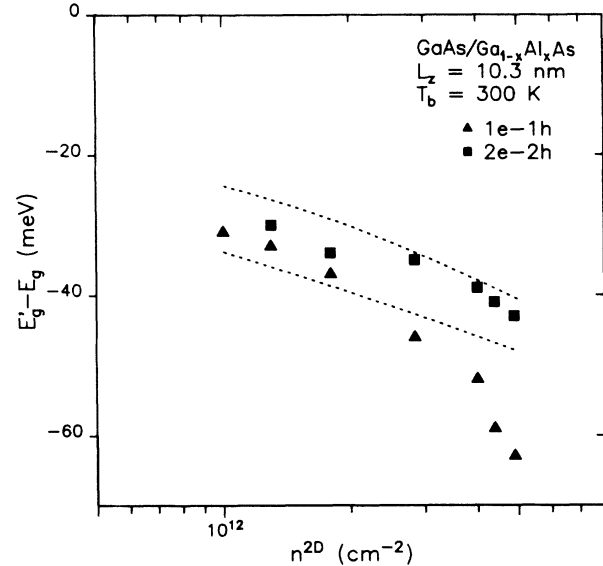


FIG. 3. Density dependence of the renormalization of the transition energies for the first and second subband of a 10.3-nm GaAs/Ga_{0.63}Al_{0.37}As quantum well. Dashed lines give the theoretical results described in the text.

that matrix elements for the forbidden transitions have strong energy dependences. Those matrix elements are comparable to those for the allowed transitions within the energy range of the high-excitation spectra. For parabolic uncoupled valence bands on the other hand, the matrix elements for the allowed transitions would be constant as a function of energy, and those for the forbidden transitions would be zero.

The experimental data shown in Fig. 1 clearly indicate a subband dependence of the band gap shifts with increasing density. In particular, the first transition ($1e-1h$) shows a strong shift to lower energies with increasing density, whereas the second transition ($2e-2h$) shows less shift. We have used line-shape fits to spectra recorded at different excitation powers to determine quantitatively the density dependence of the band renormalization of the first and second subband. The subband edges at low carrier density were determined from exciton features by excitation spectroscopy. In order to determine the shifts in the energies of several transitions, the difference between the subband edge of the first electron and hole subbands ($n=1$) and that of higher transitions ($n=2,3$) were used as parameters in the fits. The shifts for heavy and light holes for a given subband index were taken to be the same.

Figure 3 displays the density dependence of the subband transition energies for the $n=1$ (triangles) and $n=2$ (squares) transitions with respect to the low-density positions of both transitions. The zero-density transition energies were determined from exciton features in the excitation spectra using an exciton binding energy of 10 and 7 meV for the excitons corresponding to the first and the second subbands. We observe a significant difference between the renormalization of the transition energies of the different subbands. In particular, for densities of the order of $4-5 \times 10^{12} \text{ cm}^{-2}$, the renormalization of the ($1e-$

1h) transition is approximately 40% larger than for the ($2e-2h$) transition.

In bulk semiconductors the shift of the electron-hole transition energy with increasing carrier densities arises from the shifts in the single-particle self-energies due to exchange-correlation effects.⁸ In order to illustrate the origin of the subband dependence of the transition energies in a quantum-well geometry we have introduced a simple model with exchange-correlation potentials of the forms given by Hedin and Lundquist⁹ in the Kohn-Sham equations for the electrons and holes. The density dependence of these potentials was obtained from numerical results for three-dimensional systems,¹⁰ and the length and energy scales are taken to be those appropriate for the quantum-well system. The finite potential barriers were taken to be those of the sample studied here, and the Kohn-Sham equations for the single-particle energies were solved fully self-consistently at finite temperatures. Details of these calculations will be given elsewhere. Our results are in qualitative agreement with calculations in the random-phase approximation.¹¹

The resulting transition energies for the $n=1$ and the $n=2$ electron-hole transitions are shown by dashed lines in Fig. 3. Physically, the reason for the different shifts for the two transition energies is that the exchange-correlation potentials and thus the self-energies are determined by the local carrier densities. The $n=1$ -subband envelope wave functions have no nodes in the direction perpendicular to the well and are concentrated in the

center of the well, whereas the $n=2$ -subband wave functions have one node and are concentrated towards the edges of the wells. Thus an $n=1$ carrier interacts strongly with the high-density $n=1$ carriers, but an $n=2$ carrier interacts less strongly with the high density of $n=1$ carriers. This simple model gives a splitting between the $n=1$ and $n=2$ transitions, as seen experimentally. The overall magnitude of the exchange-correlation shifts also is in good accord with experiment. The density dependence of the shifts and of the splittings between the $n=1$ and $n=2$ transitions are fully accounted for by this simple model.

In summary, the emission from high-density electron-hole plasmas has been investigated in a GaAs/Ga_{1-x}Al_xAs quantum well. Uniform high carrier densities have been obtained by performing experiments on mesa structures. Accurate values of the carrier densities have been obtained by making line-shape fits using the full coupled-valence-band structures. Detailed results for the subband dependence of the band-gap shifts were obtained. Theoretical results have been presented for the band-gap shifts which show a subband dependence, which is consistent with the experimental findings.

We acknowledge stimulating discussions with M. Pilkuhn and G. Tränkle. The financial support of the Deutsche Forschungsgemeinschaft and of the Office of Naval Research is gratefully appreciated.

*Present address: Department of Physics, Boston College, Chestnut Hill, MA 02167.

†Present address: Forschungsinstitut der Deutschen Bundespost, Darmstadt, Federal Republic of Germany.

¹G. Tränkle, H. Leier, A. Forchel, H. Haug, C. Ell, and G. Weimann, *Phys. Rev. Lett.* **58**, 419 (1987).

²V. D. Kulakovskii, E. Lach, A. Forchel, and D. Grützmacher, *Phys. Rev. B* **40**, 8087 (1989).

³M. Altarelli, *J. Lumin.* **30**, 472 (1985).

⁴D. A. Broido and L. J. Sham, *Phys. Rev. B* **31**, 888 (1985).

⁵J. Vilms and W. E. Spicer, *J. Appl. Phys.* **36**, 2815 (1965).

⁶P. T. Landsberg, *Phys. Status Solidi* **15**, 623 (1966).

⁷H. Yoshimura, G. E. W. Bauer, and H. Sakaki, *Phys. Rev. B* **38**, 10791 (1988).

⁸T. M. Rice, *Solid State Physics*, edited by F. Seitz, D. Turnbull, and H. Ehrenreich (Academic, New York, 1977), Vol. 32, p. 1.

⁹L. Hedin and B. I. Lundquist, *J. Phys. C* **4**, 2064 (1971).

¹⁰P. Vashista and R. K. Kalia, *Phys. Rev. B* **25**, 6492 (1982).

¹¹C. Ell and H. Haug, *Proceedings of the International Workshop NOEKS, 1989* [*Phys. Status Solidi (b)* **159**, 117 (1990)].